OPTIMIZATION OF GRINDING PARAMETER WHEN GRIND HAYNES 242 USING WATER BASED TITANIUM OXIDE (TiO_2) NANOCOOLANT

SANGEETHA A/P GOVINDASAMY

UNIVERSITI MALAYSIA PAHANG

OPTIMIZATION OF GRINDING PARAMETER WHEN GRIND HAYNES 242 USING WATER BASED TITANIUM OXIDE (TiO_2) NANOCOOLANT

SANGEETHA A/P GOVINDASAMY

Report submitted in partial fulfilment of the requirements for the award of the degree of Bachelor of Mechanical Engineering with Manufacturing Engineering

Faculty of Mechanical Engineering
UNIVERSITI MALAYSIA PAHANG

JUNE 2012

UNIVERSITI MALAYSIA PAHANG

FACULTY OF MECHANICAL ENGINEERING

I certify that the project entitled "Optimization of Grinding Parameter When Grind Haynes 242 Using Water Based Titanium Oxide (TiO_2) Nanocoolant" is written by Sangeetha A/P Govindasamy. I have examined the final copy of this project and in my opinion; it is fully adequate in terms of scope and quality for the award of the degree of Bachelor of Engineering. I herewith recommend that it be accepted in partial fulfilment of the requirements for the degree of Bachelor of Mechanical Engineering with Manufacturing.

Signature :

Name of Panel : MR NASRUL HADI BIN JOHARI

Position :

Date :

SUPERVISOR'S DECLARATION

I hereby declare that I have checked this project report and in my opinion, this project is adequate in terms of scope and quality for the award of the degree of Bachelor of Mechanical Engineering with Manufacturing.

Signature :
Name of Supervisor : DR KUMARAN KADIRGAMA
Position :
Date :

STUDENT'S DECLARATION

I hereby declare that the work in this project is my own except for quotations and summaries which have been duly acknowledged. The project has not been accepted for any degree and is not concurrently submitted in candidature of any other degree.

Signature :

Name : SANGEETHA A/P GOVINDASAMY

ID Number : ME08040

Date :

To my beloved parents,

Mr. Govindasamy A/L Sellaiah

Mrs. Thenmoli A/P Sinnasamy

ACKNOWLEDGEMENTS

I would like to express my sincere appreciation to my Supervisor, Dr Kumaran Kadirgama for his germinal ideas, invaluable guidance, continuous encouragement and constant support in making this project possible. Without his continued support and interest, this report would not have been the same as presented here. Besides I would like to thank my co-supervisor, Prof K.V Sharma for his relentless motivation and guidance for this research project to be completed.

The next credit goes to my parents Mr. Govindasamy and Mrs. Thenmoli and also my beloved siblings for their endless support and encouragement throughout this period. I would like to thanks all my colleagues whom help me a lot in completing the project and thesis. Their friendship spirits and wise advice keep me on the right track all the time .My sincere thanks also go to all my labmates and members of the staff of the Mechanical Engineering Department, UMP who helped me in many ways and made my stay at UMP pleasant and unforgettable.

I hope this research project will be helpful for those who need reference in the field of grinding process. Finally I would like to express my gratefulness to all of them who involved directly or indirectly in the completion of my final year project and thesis. Thank you.

ABSTRACT

This thesis entitled Optimization of Grinding Parameter when grind Haynes 242 using water based Titanium Oxide (TiO_2) Nanocoolant. The objective of this thesis is to find optimum parameter which is the Depth of cut. The thesis also is to investigate type of surface roughness and wheel wear produced during grinding process. Haynes 242 material was used as the work piece and Titanium Oxide as Nanocoolant was used for this grinding process. The another objective of this thesis is also to develop prediction model for surface roughness and wheel wear produced using Neural Network Analysis. These studies will be done for two experimental processes which is the single pass and multi pass experiment according to different depth of cut. As result, we observed that as the depth of cut increases, the surface roughness of the material also increases. However, when compare between the single pass and multi pass experiment, we can observed that surface roughness for single pass are much higher than the multi pass experiment. As for the recommendation, in future we can conduct the experiment using different kind of concentration, various depths of cut, different passes and also different types of material.

ABSTRAK

Tesis ini yang bertajuk Pengoptimuman Parameter Pengisar apabila mengisar Haynes 242 menggunak an Titanium Oksida (TiO_2) cecair Nano. Objektif tesis ini adalah untuk mencari parameter optimum iaitu Kedalaman pemotongan. Tesis ini juga adalah untuk menyiasat jenis kekasaran pemukaan dan kehausan roda yang dihasilkan semasa proses pengisaran. Haynes 242 adalah bahan yang telah digunakan sebagai bahan kerja dan Oksida Titanium, sebagai cecair Nano digunakan untuk proses pengisaran. Objektif lain tesis ini juga adalah untuk mengembangkan model ramalan untuk kekasaran permukaan dan pemakaian roda yang dihasilkan menggunakan Artificial Neural Network. Kajian-kajian ini akan dijalankan untuk dua proses eksperimen yang pas tunggal dan pelbagai pas mengikut perbezaan kedalaman potongan. Hasilnya, kami memerhatikan bahawa apabila kedalaman pemotongan menaik, kekasaran permukaan bahan juga meningkat. Walau bagaimanapun, apabila bandingkan antara pas tunggal dan pas berbilang, kita boleh memerhatikan bahawa kekasaran permukaan untuk pas tunggal adalah lebih tinggi daripada eksperimen pas berbilang. Bagi syor itu, pada masa akan datang kita boleh menjalankan eksperimen menggunakan pelbagai jenis kaedah, pelbagai kedalaman potongan, pelbagai pas berlainan dan juga pelbagai jenis bahan.

TABLE OF CONTENTS

LIST OF TABLES

LIST OF FIGURES

LIST OF SYMBOLS

ω	Natural frequency
V	Volume
μm	Micrometer
Δ	Difference in volume
^{0}C	Celsius
^{0}F	Fahrenheit
K	Kelvin

LIST OF ABBREVIATIONS

Ra	Surface Roughness

TiO_2	Titanium Oxide
Ni	Nickel
Mo	Molybdenum
Cr	Chromium
Mn	Manganese
Si	Silicon
Al	Aluminium
C	Carbon
B	Boron
Cu	Copper
EG	Ethylene Glycol
TEM	Transmission Electron Microscopy
PWR	Pressurized Water Reactors
RPM	Revolution per Minute
H_2O	Water
Al_2O_3	Aluminium Oxide
CuO	Copper Oxide
ANN	Artificial Neural Network
SiC	Silicon Carbide

CHAPTER 1

INTRODUCTION

1.1 BACKGROUND OF STUDY

The grinding process is a wise, large and diverse area of manufacturing and tool making. This grinding process normally placed at the end of a production line for finishing parts with an excellent and fine surface finish and also to produce products with high dimensional accuracy. The most significant impact on the overall yield and productivity of the entire production line is obtained via the result and productivity of the grinding operation. Improvement of productivity and reduction in cost for the grinding process is increasing significantly through advanced optimization and control. However, the grinding process remains one of the most difficult to control manufacturing processes due to its nonlinear, complex and time varying nature. Determining desirable operating parameters and the tools of the grinding process in an industrial environment is predicated on operator experience and also by trial and errors method which often results in inconsistency in part qualities and low productivity. Grinding parameter which is the depth of cut should be optimized when doing the grinding process. This project is to optimize the grinding parameter of Haynes 242 material using water based Titanium Oxide nanocoolant. Besides, this study also is to investigate the type of surface roughness and wear produced during experimental process (Cheol W. Lee, 2000)

1.2 PROBLEM STATEMENT

Haynes 242 alloy is an age hardenable nickel-molybdenum chromium alloy which derives its strength from a long-range ordering reaction upon aging. Haynes 242 used commonly in industry because of its characteristic that combines high temperature strength, low thermal expansion and good oxidation. Different types of parameter in grinding process will give effect to the characteristic of the work piece. In this research, the grinding operation carried out to optimize the parameters to produce fine surface roughness and tool wear. The parameter used in this grinding process is depth of cut. Nanocoolant works better in term of thermal, so using nanocoolant will give better results for the grinding process.

1.3 OBJECTIVES

The objectives of this project are:-

a) To find optimum parameter which is the depth of cut
b) To investigate type of surface roughness and wear produced during grinding process
c) To develop prediction model for surface roughness and wheel wear produced using Neural Network

1.4 SCOPE/LIMITATION

In order to achieve the objectives notified earlier, the following scopes have been identified:-

a) Preparation of Titanium Oxide water based nanocoolant for grinding process
b) Conduct experiment using silicon carbide wheel.
c) Conduct grinding process for single pass (9 exp) and multi pass (9 exp).
d) To obtain prediction model for surface roughness and wheel wear produced using Neural Network.

e) Use Perthometer to measure Surface Roughness and Tachometer to control work Speed (200 rpm)

f) Use different depth of cut (5,7,9,11,13,15,17,19,21)µm for the grinding process.

1 .5 THESIS OUTLINE

This thesis consists of five chapters. Chapter 1 gives the introduction of this project. In this introduction part, there will be brief explanations about the background of this study, the problem statement, the objective of this study, and the scope/limitation in this project. This chapter is as a fundamental for the project and act as a guidelines for project research completion.

Chapter 2 discuss about the literature review of this project. Literature review will be mainly discussed on the Grinding machining process, Surface Machining Process, Material of work piece, Nanocoolant Properties, Titanium Oxide Nanocoolant and Thermal Conductivity of TiO_2

Chapter 3 describes the methodology part of the study. Methodology gives information about the design of experiment, experimental setup, equipment used for the grinding process and process flow of the experiment.

Chapter 4 discuss about the result and discussion part of the study. The result for surface roughness and wheel wear produced will be analyzed. Hence, the objective of this project will be achieved in this chapter.

Chapter 5 will give the overall conclusion of the project. The conclusion made will be based on the experiment and result analysis. Recommendation will be provided based on the experience during the grinding process.

CHAPTER 2

LITERATURE REVIEW

2.1 INTRODUCTION

This chapter is discussing on some literatures review which related to the optimization of grinding parameter of Haynes 242 using water based Titanium Oxide Nanocoolant. Literature review will be mainly discussed on the Grinding machining process, Material of work piece, Nanocoolant Properties, Titanium Oxide Nanocoolant and Thermal Conductivity of TiO_2

2.2 GRINDING MACHINING PROCESS

Grinding is an abrasive machining process which uses a grinding wheel as a cutting tool for finishing process. There are many types of grinding operation in Grinding machining process such as Surface grinding, Cylindrical grinding, Centerless grinding, Creep-feed grinding, Electrochemical grinding and also other grinding processes. In this research, Surface Grinding will be used for this machining process. Surface grinding is used to produce an excellent and smooth finish on flat surfaces. It is a widely used abrasive machining process in which a spinning wheel covered in rough particles (grinding wheel) cuts chips of metallic or non metallic substance from a work piece, making a face of it flat or smooth (P. Krajniket.al, 1999)

2.2.1 Surface Grinding Machine

Surface grinding is the most common of the grinding operations. It is a finishing process that uses a rotating abrasive wheel function to smooth the flat surface of metallic or nonmetallic materials to give them a more refined look or to attain a desired surface for a functional purpose. The surface grinder is composed of an abrasive wheel, a work holding device known as a chuck and a reciprocating table. The chuck holds the material in place while it is being worked on. The metallic pieces are held in place by a magnetic chuck, while nonmetallic pieces are vacuumed in place. Factors to consider in surface grinding are the material of the grinding wheel and the material of the piece being worked on. The grinding wheel is not limited to just a cylindrical shape, but can have a myriad of options that are useful in transferring different designs to the object being worked on (P. Krajniket.al, 1999)

Figure 2.1: Surface Grinding Machine

Source: Grinding Lab, University Malaysia Pahang

2.2.2 Types Of Surface Grinding

a) Horizontal-spindle (peripheral) surface grinders

The periphery (flat edge) of the wheel is in contact with the work piece, producing the flat surface. Peripheral grinding is used in high-precision work on simple flat surfaces, tapers or angled surfaces, slots, flat surfaces next to shoulders recessed surfaces and profiles. (Rogelio et al, 2003)

b) Vertical-spindle (wheel-face) grinders

The face of a wheel (cup, cylinder, disc, or segmental wheel) is used on the flat surface. Wheel-face grinding is often used for fast material removal, but some machines can accomplish high-precision work. Indexing allows loading or unloading one station while grinding operations are being performed on another. The work piece is held on a reciprocating table, which can be varied according to the task or a rotary-table machine with continuous or indexed rotation. (Rogelio et al, 2003)

c) Disc grinders and double-disc grinders

Disc grinding is similar to surface grinding but with a larger contact area between disc and work piece. Disc grinders are available in both vertical and horizontal spindle types. Double disc grinders work both sides of a work piece simultaneously. Disc grinders are capable of achieving especially fine tolerances (Rogelio et al, 2003)

2.3 GRINDING PARAMETER

The relevant variable for the grinding process is the cutting parameter (depth of cut) work piece geometry (initial surface texture and form errors) wheel topography and vibration (Y. Wang et al, 1998). Grinding parameter used in this study is Depth of cut.

2.3.1 Depth of Cut

Depth of cut refers to the distance of the grinding wheel penetrates into the work piece. When the cutting depth is big, the work speed becomes faster and thus increases the surface temperature. The surface roughness of the work piece also will be changed (Kwak J.S., 2004)

2.4 MATERIAL OF WORKPIECE

Haynes 242 alloy is an age hardenable nickel-molybdenum chromium alloy which derives its strength from a long-range ordering reaction upon aging. It has tensile and creep strength properties up to 1300^0F (705^0C) which are as much as double those for solid solution strengthened alloys but with high ductility in the aged condition. Haynes 242 alloy exhibits significantly lower thermal expansion characteristics than most nickel-base high temperature alloys in the range of temperature from room temperature to 1600^0F (8700C) and it has very good oxidation resistance up to 1500^0F (815^0C).

Haynes 242 alloy has very good forming and welding characteristics in the annealed condition. It may be forged or otherwise hot-worked by conventional techniques and it is readily cold formable. Haynes 242 alloy is furnished in the annealed condition, unless otherwise specified. The alloy is usually annealed in the range of 1900-2050^0F (925-1120^0C) depending upon specific requirements, followed by an air cool (or more rapid cooling) before aging (Haynes International, Inc)

Haynes 242 alloy is produced in the form of reforge billet, bar, plate, sheet, and wire welding products in all various sizes. Haynes 242 alloy combines properties which make it ideally suited for a variety of component applications in the aerospace industry. It will be used for seal rings, containment rings, duct segments, casings, fasteners, rocket nozzles, pumps and many others (M.K. Miller et.al)

In the chemical process industry, 242 alloys will find use in high-temperature hydrofluoric acid vapour containing processes as a consequence of its excellent resistance to that environment. The alloy also displays excellent resistance to high temperature fluoride salt mixtures. The high strength and fluorine environment resistance of 242 alloys has also been shown to provide for excellent service in fluoroelastomer process equipment, such as extrusion screws. Table 2.1 shows the chemical composition of Haynes 242 (Stephen D. Antolovich, 2000)

Table 2.1: Chemical Composition (%) of Haynes 242

Chemical Composition (%) of Haynes 242	
Ni	65.0
Mo	25.0
Cr	8.0
Fe	2.0
Co	2.5
Mn	0.8
Si	0.8
Al	0.5
C	0.03
B	0.006
Cu	0.5

Haynes 242 alloy derives its age-hardened strength from a unique long range ordering reaction which essentially doubles the un-aged strength while preserving excellent 2000 by Haynes International, Inc. ductility. The ordered Ni_2 (Mo, Cr)-type domains are less than a few hundred Angstroms in size, and are visible only with the use of electron microscopy (Haynes International. Inc)

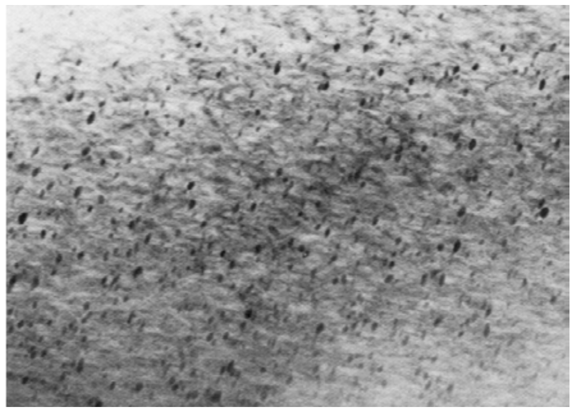

Figure 2.2: Transmission electron micrograph showing long-range-ordered (dark lenticular particles) in 242 alloys

Source: Dr. Vijay Vasudevan, University of Cincinnati

Table 2.2: Typical room temperature physical properties

	British Units	Metric Units
Density	0.327 lb/in^3	9.06 g/cm^3
Electricity Resistivity	48.0 μ ohm-in	122.0 μ ohm-cm
Dynamic modulus of Elasticity	33.2 x 10^6 psi	229 Gpa
Thermal Conductivity	75.7 Btu-in/ft^2-hr-°F	11.3 W/m-K
Specific Heat	0.092 Btu/lb.-°F	386 J/Kg-K

2.4 NANOCOOLANT

Nanocoolant can be considered to be the next-generation heat transfer fluids as they offer exciting new possibilities to enhance heat transfer performance compared to pure liquids. They are expected to have superior properties compared to conventional heat transfer fluids, as well as fluids containing micro-sized metallic particles. The much larger relative surface area of nanoparticles, compared to those of conventional particles, should not only significantly improve heat transfer capabilities but also should increase the stability of the suspensions.

Moreover, nanocoolants can improve abrasion-related properties as compared to the conventional fluid mixtures. Successful employment of nanocoolants will support the current trend toward component miniaturization by enabling the design of smaller and lighter heat exchanger systems. Keblinski et al made an interesting simple review to discuss the properties of nanocoolants and future challenges. The development of nanocoolants is still hindered by several factors such as the lack of agreement between results, poor characterization of suspensions, and the lack of theoretical understanding of the mechanisms. Nanocoolant are produced by dispersing nanometer-scale solid particles into base liquids such as water, ethylene glycol (EG) and oils (Stephen U. S. Choi, 2000)

2.5.1 Size Matters in Nanocoolant

Before diving into the specifics of the thermal properties of nanotechnology-based HTFs, it is important to understand the importance of particle size in creating practical nanocoolants. First of all, particle size matters in making nanocoolants stable. Dense nanoparticles can be suspended in liquids because the particles have an extremely high ratio of surface area to volume so that the interaction of the particle surface with the liquids is strong enough to overcome differences in density example the gravity effect is negligible. Furthermore, nanoparticles are charged and thus particle interactions are not allowed. Second, size matters in making nanocoolants with novel properties. The very small particle size can affect transport mechanisms at the nanoscale. The properties of nanocoolants are dominated not only by the characteristics of nanoscale surface or interface structures but also by nanoscale dynamics (Stephen U. S. Choi, 2000)

2.5.2 Making Nanocoolants

Dispersing the nanoparticles uniformly and suspending them stably in the host liquid is critical in producing high-quality nanocoolants. Good dispersion and stable suspension are prerequisites for the study of nanocoolants properties and for applications. The key in producing extremely stable nanocoolants is to disperse mono sized nanoparticles before they agglomerate. Many two-step and one-step physical and chemical processes have been developed for making nanocoolants. These processes can be summarized as follows:-

• *Two-step process*

In a typical two-step process, nanoparticles, nanotubes, or nanofibers are first produced as a dry powder by physical or chemical methods such as inert gas condensation and chemical vapour deposition. This step is followed by powder dispersion in the liquid. The major problem with two-step processes is aggregation of nanoparticles. Kwak, K. and Kim, C, 2005 showed that particles, strongly aggregated before dispersion, are still in an aggregated state after dispersion in ethylene glycol. Most researchers purchase nanoparticles in powder form and mix them with the base fluid.

However, these nanocoolants are not stable, although stability can be enhanced with pH control and/or surfactant addition. Some researchers purchase commercially available nanocoolants. But these nanocoolants contain impurities and nanoparticles whose size is different from vendor specifications. Although the two-step process works fairly well for oxide nanoparticles, it is not as effective for metallic nanoparticles (A.K. Singh)

• *One-step process*

In a one-step process, synthesis and dispersion of nanoparticles into the fluid take place simultaneously. For example, Argonne developed a one-step nanocoolant production system in which nanoscale vapour from metallic source material can be directly dispersed into low vapour pressure fluids (A.K. Singh)

2.5.3 Characterizing Nanocoolants

Good methods for characterizing nanocoolants are critical to a correct understanding of their novel properties. Characterization of nanocoolants includes determination of colloidal stability, particle size and size distribution, concentration, and elemental composition as well as measurements of thermophysical properties. For some applications, measurement of the electrical conductivity of nanocoolants is required. Some of the most commonly used tools for characterization include transmission electron microscopy (TEM) imaging and dynamic light scattering (DLS). One of the most measured thermophysical properties is the thermal conductivity of nanocoolants. Generally, three methods are used to measure the thermal conductivity of nanocoolants such as the transient hot wire method, 3-ωmethod and the laser flash method (Stephen U. S. Choi)

2.5.4 Applications of Nanocoolants

Nanocoolants can be used in a wide range of applications wherever improved heat transfer or efficient heat dissipation is required. Major examples include electronics, automotive, and nuclear applications. The following examples give a picture of the versatility of this technology. Nanocoolants are a promising candidate for microelectronics cooling. Tsai et al used gold nanocoolants as the working fluid for meshed circular heat pipe. Their results show that, at the same charge volume, there is a significant reduction (by as much as 37%) in the thermal resistance of the heat pipe with a nanocoolant as compared with de-ionized water (A.K. Singh)

Nanocoolants have a plethora of potential applications in many automotive parts and functions, including engine coolant, automatic transmission fluid, power steering fluid, fan clutches, engine oil, power electronics, brake fluid, gear lubrication, and greases. The first commercial steps of nanocoolants technology have been made in the automobile arena. Tzeng et al. are the first to apply nanocoolants in cooling a real-world automatic power transmission system. Nuclear applications of nanocoolants appear to be very promising or perhaps the most promising of currently envisaged uses (A.K.Singh)

Nanocoolants could be used in primary systems, emergency safety systems, and severe accident management systems, with resulting benefits such as power upgrades in commercial pressurized water reactors (PWR) and enhanced safety margins during design-basis events and severe accidents. In general, nanocoolants could enhance economics and safety of nuclear reactors. They also have great potential as a coolant for safer and smaller nuclear generators in the future. Beyond these somewhat concrete possibilities lies a broad expanse of potential applications, wide open to the engineering imagination (A.K. Singh)

2.6 TITANIUM OXIDE (TiO_2)

Titanium Oxide is a widely used white pigment because of its brightness. It can also oxidize oxygen or organic materials, therefore, it is added to paints, cements, windows, tiles, or other products for sterilizing, deodorizing and anti-fouling properties and when incorporated into outdoor building materials can substantially reduce concentrations of airborne pollutants. Additionally, as TiO_2 is exposed to UV light, it becomes increasingly hydrophilic (attractive to water), thus it can be used for anti-fogging coatings or self cleaning windows.

Titanium (v) Oxide water based nanocoolant used in this project is the mixture of Rutile and Anatese which contain <150nm particle size dispersion, 33-37 ωt% in H_2O, 99.9% frace metal basis.

2.6.1 Thermal Conductivity

Thermal conductivity is an important parameter in enhancing the heat transfer performance of a base fluid. Since the thermal conductivity of solid metals is higher than that of fluids, the suspended particles are expected to increase the thermal conductivity and heat transfer performance. Many researchers have reported experimental studies on the thermal conductivity of nanocoolants. The temperature oscillation method, the steady-state parallel plate method, and transient hot-wire method have been employed to measure the thermal conductivity of nanocoolants. However, the transient hot-wire method has been extensively used by many researchers (Sridhara and Satapathy, 2011)

Published results show an enhancement in the thermal conductivity of nanocoolants, in a wide range even for the same host fluid and same nominal size or composition of the additives. Since this enhancement can't be explained with the existing classical effective thermal-conductivity models, such as the Maxwell or Hamilton–Crosser models, this also motivates a wide range of theoretical approaches for modelling these thermal phenomena. Reported results show that the particle volume concentration, particle material, particle size, particle shape, base fluid material, temperature, additive, and acidity play an important role in enhancement of the thermal conductivity of nanocoolants (A.Turgut et.al)

The effect of the fluid temperature on the effective thermal conductivity of nanoparticle suspensions was first presented by Masuda et al. They reported that for water-based nanocoolants, consisting of SiO_2 and TiO_2 nanoparticles, the thermal conductivity was not much more temperature dependent than that of the base fluid. Contrary to this result, Das et al. observed a two-to-four fold increase in the thermal conductivity of nanocoolants, containing Al_2O_3 and CuO nanoparticles in water, over a temperature range of 21 $^{\circ}$C to 51°C. Several groups reported studies with different nanocoolants, which support the result of Das et al. For the temperature dependence of the relative thermal conductivity (ratio of effective thermal conductivity of nanocoolants to thermal conductivity of base fluid), although a major group of publications showed an increase with respect to temperature, some of the other groups observed a moderate enhancement or temperature independence (A. Turgut et.al)

Below are the study conducted by A.Turgut and friends. A.Turgut et al compare the result with all others author entitled comparison of thermal conductivity enhancement in TiO_2 water nanocoolants

Table 2.3: Comparison of thermal conductivity enhancement in TiO_2 water nanocoolants

Author	Nominal TiO_2 particle size (nm)	Volume fraction (%)	Thermal conductivity enhancement (%)	Reduced thermal conductivity enhancement and temperature	Measurement method
(a) *In the literature*					
Masuda et al. [6]	27	1.00	2.0	2.0 at 32 °C	Transient hot wire
		2.00	4.8	2.4 at 32 °C	
		3.25	8.0	2.5 at 32 °C	
		3.25	8.4	2.6 at 47 °C	
		3.10	7.5	2.4 at 87 °C	
		4.30	10.5	2.4 at 32 °C	
		4.30	10.8	2.5 at 47 °C	
		4.30	9.9	2.3 at 87 °C	
Wang et al. [12]	26	0.5	1.5	3.0 at 18 °C	3 ω method
		0.5	5.0	10.0 at 65 °C	
		1.0	3.1	3.1 at 18 °C	
		1.0	6.0	6.0 at 43 °C	
		1.0	10.0	10.0 at 65 °C	
		2.0	4.6	2.3 at 18 °C	
		2.0	8.4	4.2 at 43 °C	
		2.0	13.3	6.7 at 65 °C	
		4.0	11.0	2.8 at 18 °C	
		4.0	15.0	3.8 at 43 °C	
		4.0	19.5	4.9 at 65 °C	
Zhang et al. [16]	40	0.6	1.4	2.3 at 10 °C	Transient short hot wire
		1.2	3.1	2.6 at 10 °C	
		2.6	5.8	2.2 at 10 °C	
		1.2	3.6	3.0 at 30 °C	
		2.6	5.4	3.0 at 30 °C	
		0.6	1.1	2.1 at 40 °C	
		1.2	3.7	3.1 at 40 °C	
		2.6	6.5	2.5 at 40 °C	
Yoo et al. [32]	25	0.1	10.0	100	Transient hot wire
		0.5	11.8	23.6	
		1.0	14.5	14.5	
He et al. [33]	21	0.24	1.9	7.9 at 22 °C	Transient hot wire
		0.6	3.6	6.0 at 22 °C	
		1.18	7.5	6.4 at 22 °C	
		1.92	8.6	4.5 at 22 °C	
Pak and Cho [34]	27	1.0	3.5	3.5	Transient hot wire
		2.0	5.0	2.5	
		3.0	7.7	2.6	
		4.0	12.0	3.0	
Murshed et al. [35]	15	0.5	4.5	9.0	Transient hot wire
		0.8	9.5	11.9	
		1.0	18.5	18.5	
		2.0	23.5	11.8	
		3.0	25.5	8.5	
		4.0	27.5	6.9	
		5.0	30.0	5.9	

Author	Nominal TiO_2 particle size (nm)	Volume fraction (%)	Thermal conductivity enhancement (%)	Reduced thermal conductivity enhancement and temperature	Measurement method
		0.29	1.8	6.2	Transient
		0.41	3.1	7.6	hot wire
Wen and Ding [36]	34	0.53	5.1	9.6	
		0.68	6.3	9.3	
(b) *From this study*		0.2	0.4	2.0 at 13 °C	
		1.0	2.5	2.5 at 13 °C	
		2.0	4.2	2.1 at 13 °C	
		3.0	7.4	2.5 at 13 °C	
		0.2	0.3	1.5 at 23 °C	
		1.0	2.3	2.3 at 23 °C	
		2.0	4.3	2.2 at 23 °C	
Present results	21	3.0	6.9	2.3 at 23 °C	
		0.2	0.5	2.5 at 40 °C	3 ω method
		1.0	2.7	2.7 at 40 °C	
		2.0	4.8	2.4 at 40 °C	
		3.0	7.1	2.4 at 40 °C	
		0.2	0.3	1.5 at 55 °C	
		1.0	2.2	2.2 at 55 °C	
		2.0	4.5	2.3 at 55 °C	
		3.0	7.2	2.4 at 55 °C	

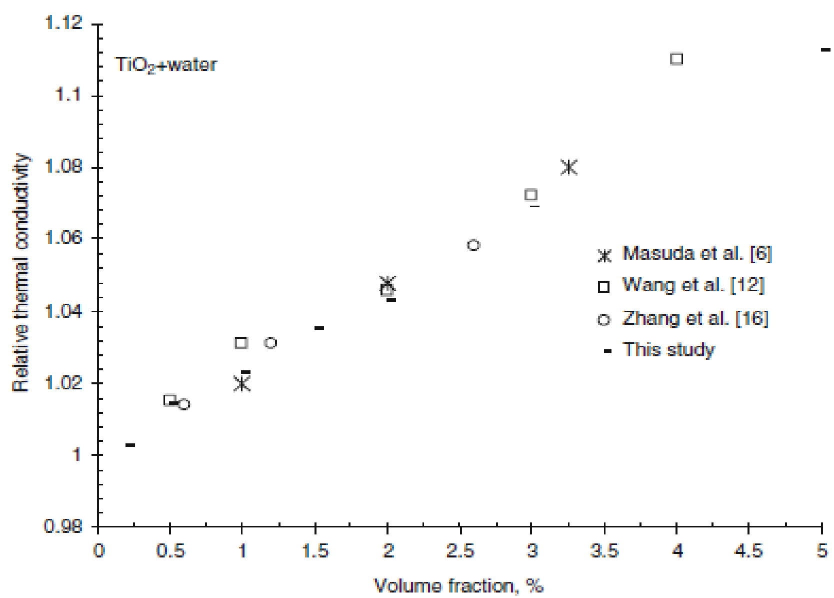

Figure 2.3: Experimental results of relative thermal conductivity of TiO_2 nanocoolants, for room temperature (23 ◦C for our data), compared to selected literature data.

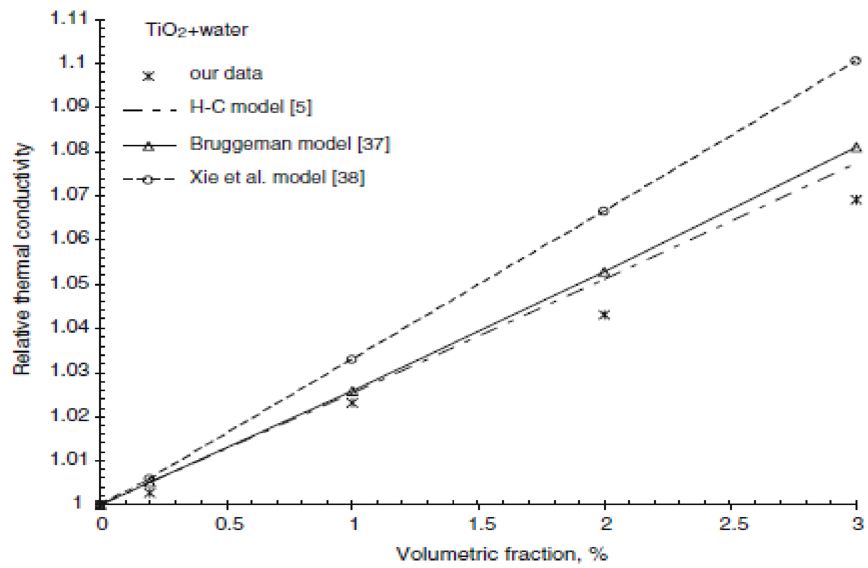

Figure 2.4: Experimental data for the relative thermal conductivity of TiO_2 nanocoolants from this study, compared to models

2.6.2 Viscosity

Viscosity is the one of properties that is needed to know to determine heat transfer rate of fluid. Viscosity is a scientific term describing the internal friction of a fluid or gas. Both have adjacent layers, and when pressure is applied, the friction between layers affects how much the substance will respond to external force. Yunus A. Cengel, (2006) said in his book, viscosity, in its simplest form, can be evaluated by the thickness of a substance. A general rule is that gases are less viscous than liquids, and thicker liquids exhibit higher viscosity than thin liquids (Mohd Taufiq, 2010)

Turgut et al., 2009 have conducted experiments to determine the viscosity of TiO_2 nanoparticles in deionised water for volume concentration up to 3%. The temperature range of experimentation is between 13 and 55°C with particles having a mean diameter of 21nm.The viscosity of nancoolants increased drastically with concentration at 13°C. The enhancement in viscosity is observed to be 7.4 % higher than the base fluid at 3% concentration.

2.6.3 Neural Network

Neural networks are non-linear mapping systems that consist of simple processors, which are called neurons, linked by weighted connections. Each neuron has inputs and generates an output that can be seen as the reflection of local information that is stored in connections. The output signal of a neuron is fed to other neurons as input signals via interconnections. Since the capability of a single neuron is limited, complex functions can be realized by connecting many neurons. It is widely reported that structure of neural network, representation of data, normalization of inputs–outputs and appropriate selection of activation functions have strong influence on the effectiveness and performance of the trained neural network. (Aisyah, 2006)

An Artificial Neural Network (ANN), usually called neural network (NN), is a mathematical model which is inspired by the structure and functional aspects of biological neural networks. A neural network consists of artificial neurons, and it processes information using a connectionist approach to computation. In most cases an ANN is an adaptive system that changes its structure based on external or internal information that flows through the network during the learning phase. Modern neural networks are non-linear statistical data modelling tools. They are usually used to model complex relationships between inputs and outputs or to find patterns in data.

On the other hand, there are very few publications appeared in the literature for predicting surface roughness utilizing neural network modelling. In an earlier work, Azouzi and Guillot examined the feasibility of neural network based sensor fusion technique to estimate the surface roughness and dimensional deviations during machining. This study concludes that depth of cut, feed rate, radial and z-axis cutting forces are the required information that should be fed into neural network models to predict the surface roughness successfully (Aquino et al, 2007)

A neural network consists of at least three layers which is input, hidden and output layers, where inputs (pi) applied at the input layer and outputs (ai) are obtained at the output layer and learning is achieved when the associations between a specified set of input–output (target) pairs. The examples of training algorithm are Quick propagation, Conjugate Gradient Descent, Quasi Newton, Limited Memory Quasi Newton, Levenberg-Marquardt, Online Back Propagation and Batch Back Propagation. Quick Propagation is a heuristic modification of the standard back propagation algorithm. It was introduced by Fahlman in 1988(Aquino et al, 2007)

CHAPTER 3

METHODOLOGY

3.1 INTRODUCTION

This chapter introduces the experimental procedure or methodology utilized to study about the surface roughness which will perform step by step that will be done during this project. This project is being done to find the various result for surface roughness of Haynes 242 material after undergoes grinding process. This will be studied using different depth of cut.

3.2 DESIGN OF EXPERIMENT

To proceed with the experiment, first we must design the experiment flow. This design include the equipment used, material used and all the preparation we done to obtain a result. For example, we must classify type of wheel used, the specification of grinding machine and also the preparation of nanocoolant.

3.2.1 Wheel properties

Grinding wheel consists of hard abrasive grains called grits, which perform the cutting or material removal, held in the weak bonding matrix. A grinding wheel commonly identified by the type of the abrasive material used (L, M karagphur, 1999). For this experiment, silicon carbide was used as a grinding wheel. Silicon carbide is harder than alumina but less tough. Silicon carbide is also inferior to Al_2O_3because of its chemical reactivity with iron and steel. Moreover, silicon carbide is a material with low density, low thermal expansion, excellent thermal shock resistance, good chemical resistance, high hardness and wears resistance. Other than that, Silicon Carbide, SiC contain outstanding thermal conductivity properties and resistance to fluctuations in temperature.

Figure 3.1: Silicon Carbide Wheel

3.2.2 Grinding Machine Specification

For this experiment, surface grinding machine are used for grinding process. Surface grinding machine can be classified into a few models. For this process, model supertech was used. The model name is STP-1022 ADCII. This machine can be used automatically and also manually. The table 3.1 shows the specification of supertech grinding machine and figure 3.2 shows the surface grinding machine.

Table 3.1: Specification of Supertech Grinding Machine

Vertical feed least count	0.01mm
Micro feed least count	0.002mm
Cross feed least count	0.05mm
Height from table to grinding wheel	275mm
Working surface of the table	300mm x 600mm
Size of the grinding wheel	200mm x 20mm x 31.75mm
Spindle Speed	2800rpm
Electric Motor Recommended	2HP-2800rpm

Figure 3.2: Supertech Surface Grinding Machine

3.2.3 Preparation of Nanocoolant

To proceed with the grinding process, nanocoolants for grinding operation should be prepared first. So, in this research Titanium Oxide used as water based nanocoolant. Preparation of nanocoolant is done step by step. First, nanocoolant new tank is prepared, followed by the preparation of distilled water and the dilution process of nanocoolant.

3.2.3.1 Preparation of Nanocoolant New Tank

The purpose of the new tank is because the normal tank provided are very big and need large amount of nanocoolant. So we prepare a tank which can be filled up with 30 litre of nanocoolant. A new coolant pipe, filter and pump were also used to prepare a new tank.

3.2.3.2 Preparation of Distilled Water

First, on the main switch and distilled water power supply of Aquamatic Water Still. The water level in the heater must be above the top level. Water vaporized in the metal heater. Later, the steam of vaporized water will be cooled by boron silica glass. The cooled water will be supplied as distill water to the distill water tank.

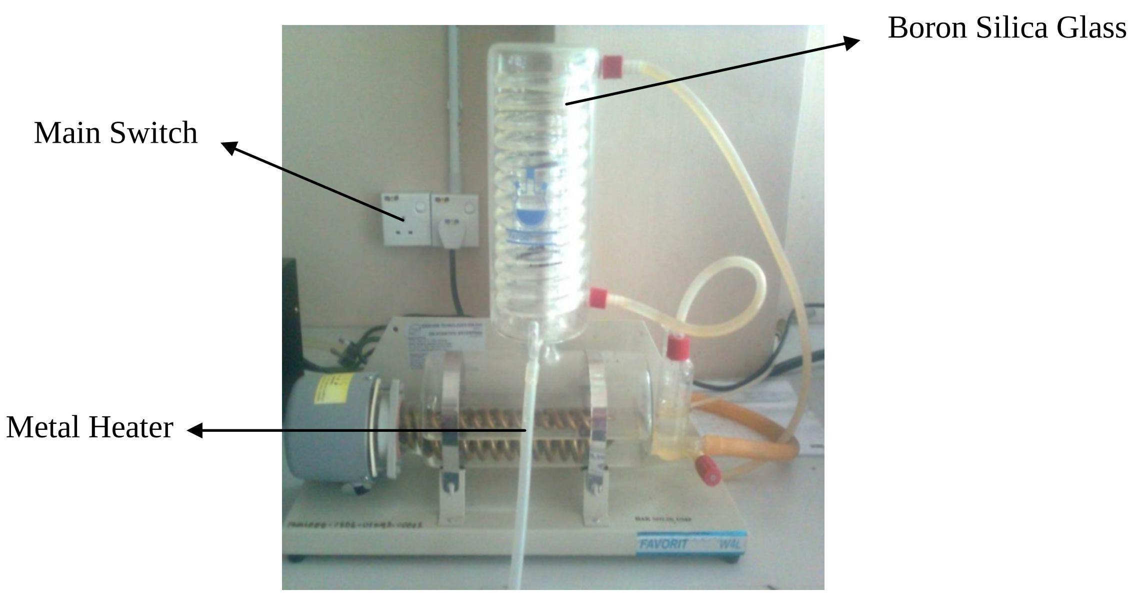

Figure 3.3: Aquamatic Water Still

Figure 3.4: Distilled Water Prepared

3.2.3.3 Calculation Of Titanium Oxide Concentration

Titanium (v) Oxide water based nanocoolant used in this project is the mixture of Rutile and Anatese which contain <150nm particle size dispersion, 33-37 ωt% in H_2O, 99.9% frace metal basis. 3 bottles of Titanium Oxide is mixed and the total volume is 220ml.

Table 3.2: Concentration of Titanium Oxide in Weight and Volume Percentage

Type of Nanocoolant	**Diameter (nm)**	**Concentration (w.w)%**	**Concentration (v.v)%**
TiO_2	150	35	11.42

Expression for conversion ωt, ø to vol, ø

The nanocoolant is procured from Sigma-Aldrich which are available in weight concentration and listed in Table 3.1. The nanocoolant concentration in weight percent, ω is converted into volume percent using Eq. (3.1 and 3.2)

$$\phi = \frac{\omega\rho_w}{\left(1-\frac{\omega}{100}\right)\rho_p + \frac{\omega}{100}\rho_w} \qquad (3.1)$$

$$\phi = \frac{\phi\rho_w}{(1-\phi)\rho_p + \phi\rho_w} \qquad (3.2)$$

$$\phi_1 = \frac{0.35(1000)}{(1-0.35)(4175) + (0.35)(1000)}$$

$$\phi_1 = 0.1142 \text{ volume}$$

3.2.3.4 Dilution Process

For the dilution process, one step preparation will take place. In one step process, synthesis and dispersion of nanoparticles into the fluid take place simultaneously. The 220ml of Titanium Oxide will be diluted with 14 litre of distill water. The equipment used in this dilution process is motorized stirrer machine, pail, 500ml beaker and 14 of litre of distill water. First, the 7 litre of distill water measured and poured into the pail which already set with the motorized stirrer machine. Later, the titanium oxide will be added slowly to the pail. After adding TiO_2, another 7 litre of distill water will added to the mixture. Later, the mixture will be diluted to 0.10 volume % concentration. So for that, another 10 liter of distill water will be added. So overall the volume will be around 25 litre. The mixture of TiO_2 and distill water will be stirred for 1 hour with the speed of 1000rpm.

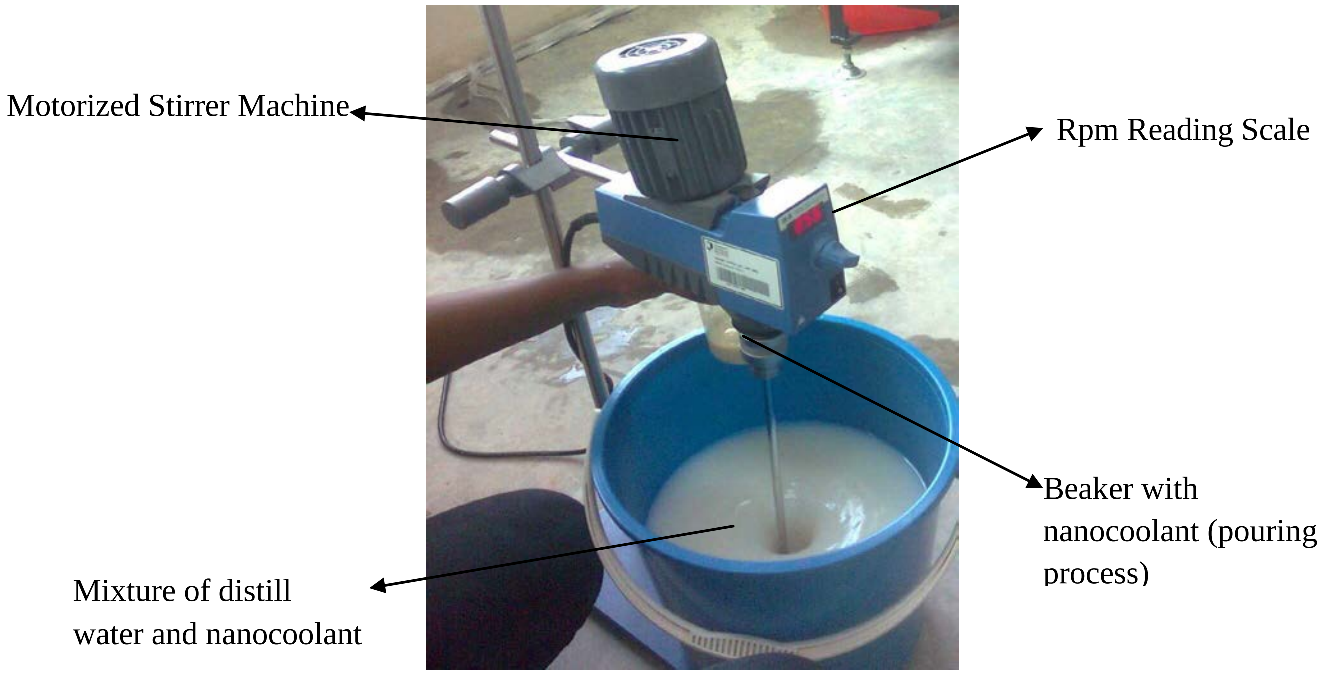

Figure 3.5: Dilution Process

<u>Expression for Total Amount Distill Water to be added</u> :-

The required volume concentration can be estimated by adding water to the existing nanocoolant available in volume percent concentration using the relations given by Eq. (3.3).

$$\Delta V = V_1\left(\frac{\phi_1}{\phi_2} - 1\right) \tag{3.3}$$

Where, $\Delta V = V_2 - V_1$; volume of DW into the nanocoolant

V_1; initial volume

V_2; final volume

ϕ_1; Volume percent before dilution

ϕ_2; Volume percent after dilution

ΔV = 14000mldistill water

V_1 = 220ml

ϕ_1 = 0.1142 volume

$$\Delta V = V_1\left(\frac{\phi_1}{\phi_2} - 1\right)$$

$$14000 = 220\left(\frac{0.1142}{\phi_2} - 1\right)$$

= 1.7668073 x 10^{-3} volume

ϕ_2 = 0.17668073 volume %

The volume of 14220ml of titanium oxide with the concentration of 0.17668073 volume percentage is obtained. Later, the nanocoolant with the concentration of 0.17668073 volume % will be diluted again for the concentration of 0.10 volumes.

$$\Delta V = V_1\left(\frac{\phi_1}{\phi_2} - 1\right)$$

V_1 = 14220ml

ϕ_1 = 0.17668073vol%

ϕ_2 = 0.10 volume

$$\Delta V = 14220 \left[\frac{0.17668073}{0.10}\right] - 1$$

ΔV = 10903.99 ml

From the calculation above, 10903.99 ml of distil water need to be added to get a solution with the concentration of 0.10 volume percentage.

$\Delta V = V_2 - V_1$

$10904 = V_2 - 14220$

$V_2 = 25124$ml

25 Litre of nanocoolant and distill water mixture obtained.

3.2.3.5 Nanocoolant Prepared

Finally, 25124ml of Titanium Oxide Nanocoolant with the concentration of 0.10 volume % was prepared.

Figure 3.6: Titanium Oxide Nanocoolant Prepared

3.3 PROPERTIES OF TiO_2 NANOCOOLANT

The thermal conductivity of nanocoolant was measured using KD2 Pro thermal property analyzer (Decagon Devices, Inc., USA). It consists of a handheld controller (microcontroller and power control) and three separate sensors (heating element and thermistor) for solid and liquid. The thermal conductivity measurement assumes the long heat source can be treated as an infinite line heat source. The sample medium is isotropic and homogeneous solution. The initial temperature of the sample is assumes constant. Even though the assumptions are not reflecting to the real measurement condition, they are sufficient for accurate thermal conductivity measurements.

The KS-1 sensor needle was used in the thermal conductivity measurement. It was made by stainless steel with 60 mm long and 1.3 mm diameter. The sensor needle dimension is closely approximates the infinite line heat source which gives least disturbance to the sample during measurements. It is designed primarily for liquid samples in the range of 0.2 to 2.00 W/m.K with an accuracy of ±5%. The KD2 Pro uses the transient line heat source method to measure thermal properties of fluid sample. The KD2 Pro takes measurements at 1-second intervals during a 90-second measurement cycle. A 30 second heat pulse is applied to a needle, and the temperature response with time is monitored either at the heated needle or at an adjacent needle. During the first 30 s, the instrument will equilibrate which is then followed by heating and cooling of sensor needle for 30 s each. It then analyzes the data and corrects for sample temperature drift to providing accurate thermal properties measurements. At the end of the reading, the controller computes the thermal conductivity using Eq. (3.4).

$$k = \frac{q\left[\ln(t_2) - \ln(t_1)\right]}{4\boldsymbol{\pi}(\Delta T_2 - \Delta T_2)} \qquad (3.4)$$

where q is constant heat rate applied to an infinitely long and small "line" source, ΔT_1 and ΔT_2 are the changes in the temperature at times t_1 and t_2, respectively.

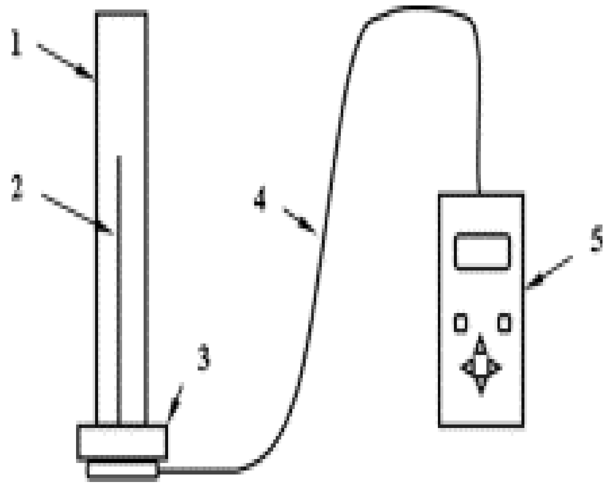

Figure 3.7: KD2 image

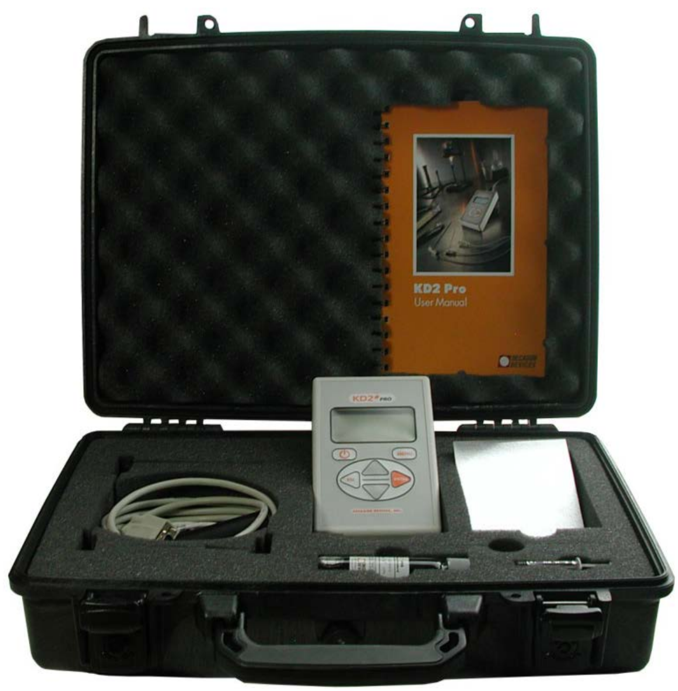

Figure 3.8: KD2 Pro transient hotwire thermal conductivity meter

The steps taken to minimize both forced and free convection heat transfer in the measured sample:-

i) Ensure that there is no shaking, mixing, or vibration of the fluid during or immediately before the measurement.

ii) Vertical insertion of the probe into the fluid will minimize errors from free convection.

iii) Less viscous fluids are more subject to errors from free convection. Low viscosity fluids must be stabilized before measurement with the KD2 sensor.

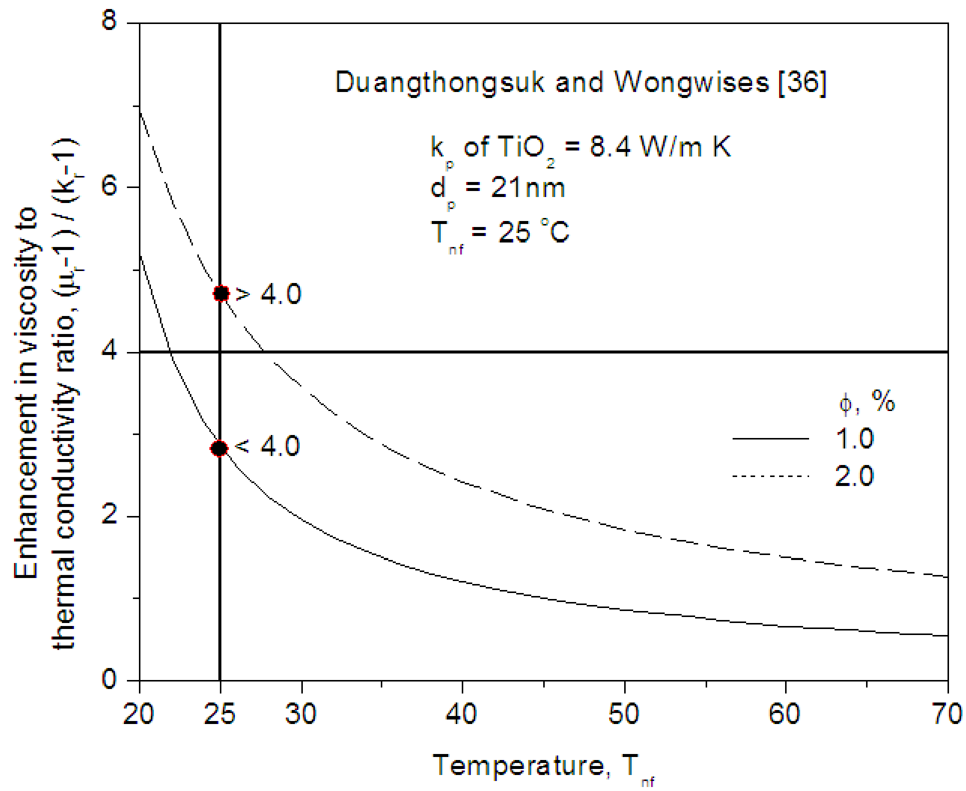

Figure 3.9: Variation of property enhancement ratio with temperature for TiO_2

3.4 EXPERIMENTAL SETUP

3.4.1 Nanocoolant setup

After preparing titanium oxide nanocoolant as explain earlier, the 25 litre of nanocoolant is filled into 30 litre tanks. Later a new setup of coolant tank is produced. New coolant pipe is fixed into the grinding machine. The nanocoolant will flows into the pipe which finally enters back to the 30 litre tank.

Figure 3.10: Nanocoolant pipe fixing

3.4.2 Grinding process

i) After filling in the nanocoolant, the rest of the material and equipment should be prepared also.

ii) The diameter of the grinding wheel, silicon carbide will be measured first. The wheel is cleaned up using wheel dressing. After that, grinding wheel will be positioned into the grinding machine.

iii) To operate the grinding machine, we must test the grinding process using other work piece first. We must use hand wheel to set up.

iv) Then, clamped our own work piece and set grinding wheel properly. Later, set the depth of cut. After setting the depth of cut, check again the work piece and grinding wheel. All should be positioned properly.

v) Start operate the machine and on the coolant. The speed should be controlled.

vi) These process is repeated for different depth of cut (5,7,9,11,13,15,17,19,21)µm. The material will be tested with single pass and multi pass. After run the experiment, the coolant flow will be closed. The machine will be off mode.

vii) Later, the surface roughness of the work piece is measured using Perthometer according to different depth of cut. The result of 2D Microstructure will be taken also.

viii) All the result obtained will be analyzed later using neural network analysis. In Network Training Option, the training algorithm used to analyze result is quick propagation. In Architecture Search Option, set R-squared for fitness criteria column. The iteration will be 500. Then, the result will be trained. To obtained better result, the iteration will be changed and above process in ANN (Artificial Neural Network) will be repeated.

ix) For example, after the training option we will obtain the result. For this experiment, we use comparison with 9 depth of cut. So 7 depths will be chosen as training set (TRN), 1 will become validation set (VLD) and another 1 will be chosen as test set (TST). After test the result, we will obtain the summary for the analysis and the correlation and R-Squared will obtained also.

Table 3.3: Example of Actual Versus Output table

	Depth of cut	Row	Target	ARE	Output	AE
TST	0	5	0.295	0.352963	0.057963	19.648485
TRN	1	7	0.348	0.355197	0.007197	2.067966
TRN	2	9	0.36	0.360438	0.000438	0.121598
VLD	3	11	0.373	0.372985	0.000015	0.004011
TRN	4	13	0.413	0.402742	0.010258	2.48381
TRN	5	15	0.454	0.461328	0.007328	1.614019
TRN	6	17	0.591	0.576856	0.014144	2.393239
TRN	7	19	0.924	0.950195	0.026195	2.834993
TRN	8	21	1.31	1.244369	0.065631	5.01002

Figure 3.11: Setting grinding machine

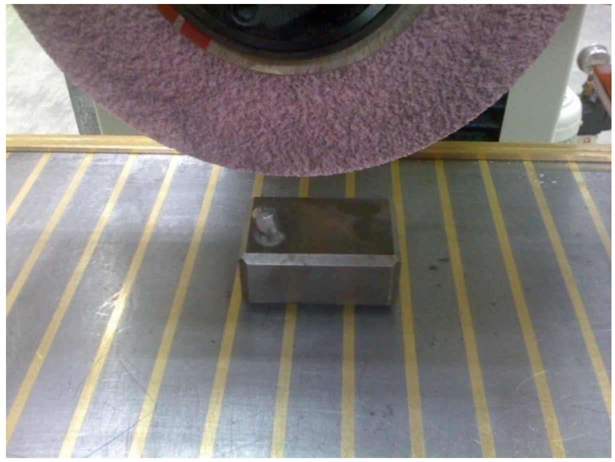

Figure 3.12: Wheel dressing

CHAPTER 4

RESULTS AND DISCUSSION

4.1 INTRODUCTION

This chapter mainly discuss about the results obtained during the experiment. The tests that have been done during this experiment are surface roughness test, wheel wear result and microstructure observations.

4.2 SURFACE ROUGHNESS MEASUREMENT

The grinding process will be run for single pass and multi pass according to different depth of cut. The surface roughness will be measured using perthometer. Three reading will be taken (initial, medium and final) for each depth of cut. Before grind the material according to the depth of cut, the surface of the material will be grind first until a smooth surface obtained.

The table 4.1 shows the result of surface roughness for single passexperiment and table 4.2 shows the result of surface roughness for multi pass experiment after grind Haynes 242 material according to the different depth of cut. Both table shows that when depth of cut increases the surface roughness also increase. This happen because when grind for a small depth of cut, the grinding forces applied on the work piece will be lower. But when increase in depth of cut, the forces applied for each depth will be increase also. When bigger forces applied, the surface produced will be rough also. Thus, surface roughness will increase. But when compare with both experiments, overall the roughness obtained for multi pass are much lesser than single pass experiment.

Figure 4.1 shows that surface roughness increases as the depth of cut increase. The graph also shows that surface roughness for single pass is higher than the surface roughness for multi pass. This is because the single pass will be run for single time only compare to multi pass experiment which will be conducted for four times. When the wheel passes by the work piece for multi experiment, it tends to be in contact with the surface of work piece for four times. Forces will be applied each time the work piece undergoes grinding process. So when grinding wheel passes by the work piece, it will grind the surface of Haynes 242 material. The more the wheel grind the work piece surface, the smoother will be surface of work piece. Finally, the surface roughness of the material for multi pass will be lower compare to single pass. Besides that, the fine and smooth surface will be obtained for multi pass experiment

Based on Adeel H. Suhail et al entitled In-process Surface Roughness Prediction Using Heat Generation Rate of work piece Surface research, he investigate that depth of cut has a much greater influence on the work piece surface temperature, and when depth of cut increase surface roughness also will increase. The surface temperature of work piece increases. Thus the higher work piece surface temperature means the rougher will be the surface roughness. Besides according to another researcher, J. Kopac et al, he investigate that, as the increase in contact of wheel to the work piece, the process power increase, the quantity of thermal energy that is introduced into the work piece also increases due to the higher forces applied. Thus, the surface roughness of the work piece will be smoother. So when compare with these experiment, forces are applied for the multi pass experiment each time the grinding wheel pass by the surface of the work piece. Thus, the more it passes on the work piece, the more fine surface roughness will be produced.

Table 4.1: Surface roughness obtained for single pass

Depth of Cut (μm)	Surface Roughness (μm)			
	Initial	**Medium**	**Final**	**Ra**
5	0.286	0.302	0.296	0.295
7	0.336	0.345	0.364	0.348
9	0.358	0.369	0.351	0.36
11	0.383	0.365	0.372	0.373
13	0.398	0.421	0.419	0.413
15	0.466	0.457	0.438	0.454
17	0.647	0.531	0.596	0.591
19	0.912	0.885	0.975	0.924
21	1.382	1.256	1.293	1.31

Table 4.2: Surface roughness obtained for multi pass

Depth Of Cut (μm)	Surface Roughness (μm)			
	Initial	**Medium**	**Final**	**Ra**
5	0.186	0.197	0.201	0.195
7	0.204	0.213	0.199	0.205
9	0.224	0.219	0.212	0.218
11	0.248	0.228	0.237	0.238
13	0.259	0.253	0.265	0.259
15	0.278	0.264	0.281	0.274
17	0.298	0.306	0.315	0.306
19	0.311	0.318	0.325	0.318
21	0.334	0.327	0.321	0.327

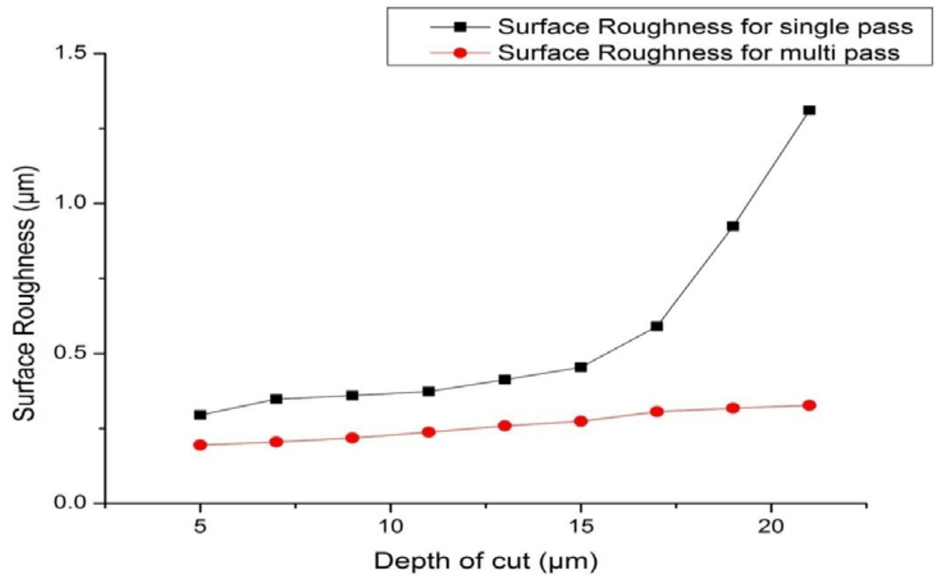

Figure 4.1: Surface Roughness for multi pass and single pass

Figure 4.2 shows graph of Surface roughness versus depth of cut for titanium oxide and water based coolant for both experiment. When comparing both result obtained, we can see that the surface roughness of water based coolant are higher than the surface roughness obtained when using Titanium Oxide. Titanium oxide nanocoolant has high thermal conductivity compare to water based coolant. Thus, when we use titanium oxide nanocoolant for grinding process, the heat dispersed will be less. So when the work piece is grind, the heat produced will be less because the nanocoolant used has high thermal conductivity. Thus the result of surface roughness using Titanium Oxide Nanocoolant will be lower than water based coolant.

Based on Emmanuel C. Nsofor, his research entitled Recent Patents on Nanocoolants (Nanoparticles in Liquids) Heat Transfer; he stated that a nanocoolant is a solid-liquid mixture produced by dispersing metallic nanoparticles in a liquid to enhance the heat transfer performance. When he did a comparison between water based coolant and nanocoolant, his experiments have shown that nanocoolants have substantial higher thermal conductivities compared to the base fluids. A number of studies have been performed to explain the reasons for the enhanced thermal performance of nanocoolants. Early attempts to predict the experimentally measured values of the thermal conductivity of nanocoolants were made with existing theories such as those by Maxwell and Hamilton-Crosser.

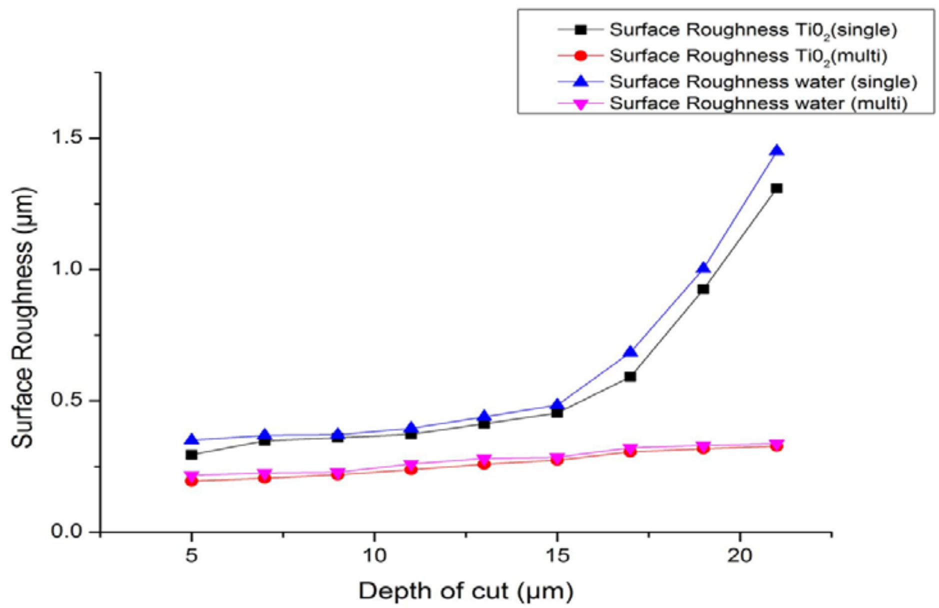

Figure 4.2: Comparison of surface roughness for TiO_2 and water based coolant

4.2.1 Microstructure Observation

From the microstructure studies, these are the results that obtained. The study on microstructure of Haynes 242 material after metal grinding process is done. The observation is done with the aid of optical measurement.

Figure 4.3(a), (b), and (c) show the observed microstructure according to the depth of cut for single pass. Figure 4.4(a), (b) and (c) shows the observed microstructure according to depth for multi pass. After took the result of surface roughness, the surface of Haynes 242 material will be seen through the optical measurement. According to the observation, roughness for multi pass is much smoother compare to the roughness for single pass. For both passes, the depth of cut for 5µm has less surface roughness.

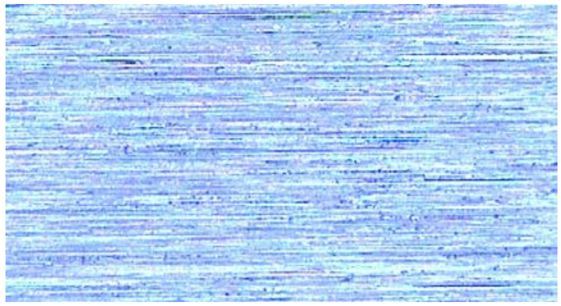

(a) 5µm

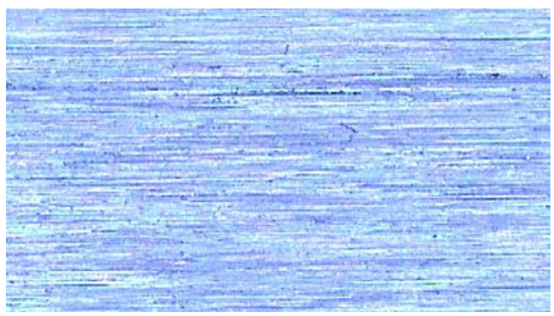

(b) 11 µm

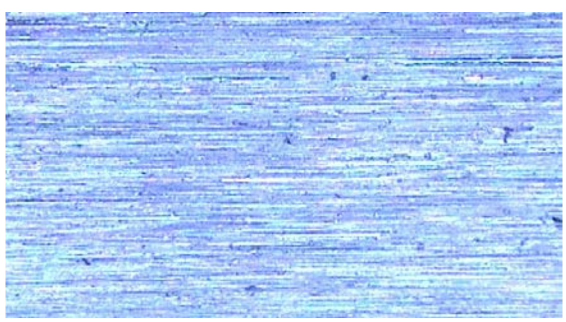

(c) 21 µm

Figure 4.3: Roughness for single pass

(a) 5µm

(b) 11µm

(c) 21µm

Figure 4.4: Roughness for multi pass

4.3 WHEEL WEAR

The table 4.3 and table 4.4 show the wheel wear result for single pass and multi pass. There is no wheel ratio obtained because there are no changes between the initial diameter and final diameter of the wheel. This is because the vernier caliper could not detect the changes in the wheel diameter. Increase in depth of cut will decrease the wheel diameter. This is because after grind the work piece for each depth, the wheel will be cleaned using wheel dressing.

Table 4.3: Wheel wear result for single pass

Depth of Cut (µm)	**Wheel Wear**		
	Wheel Diameter, d_1	**Wheel Diameter, d_2**	**Wheel ratio**
5	163.29	163.29	-
7	163.25	163.25	-
9	163.19	163.19	-
11	163.12	163.12	-
13	163.06	163.06	-
15	162.99	162.99	-
17	162.91	162.91	-
19	162.85	162.85	-
21	162.78	162.78	-

Table 4.4: Wheel wear result for multi pass

Depth of Cut (µm)	Wheel Wear		
	Wheel Diameter, d_1	Wheel Diameter, d_2	Wheel ratio
5	161.98	161.98	-
7	161.85	161.85	-
9	161.76	161.76	-
11	161.64	161.64	-
13	161.56	161.56	-
15	161.48	161.48	-
17	161.35	161.35	-
19	161.22	161.22	-
21	161.05	161.05	-

4.4 NEURAL NETWORK

4.4.1 Single Pass

Table 4.5: Target and Output Result obtain using neural network

	Row	Depth of cut	Target	Output	AE	ARE
TRN	0	5	0.295	0.304454	0.009454	3.204694
TRN	1	7	0.348	0.336338	0.011662	3.351113
TRN	2	9	0.36	0.372794	0.012794	3.55393
TST	3	11	0.373	0.395025	0.022025	5.904838
VLD	4	13	0.413	0.412898	0.000102	0.0246
TRN	5	15	0.454	0.450932	0.003068	0.675741
TRN	6	17	0.591	0.582589	0.008411	1.423204
TRN	7	19	0.924	0.95189	0.02789	3.018431
TRN	8	21	1.31	1.232731	0.077269	5.898422

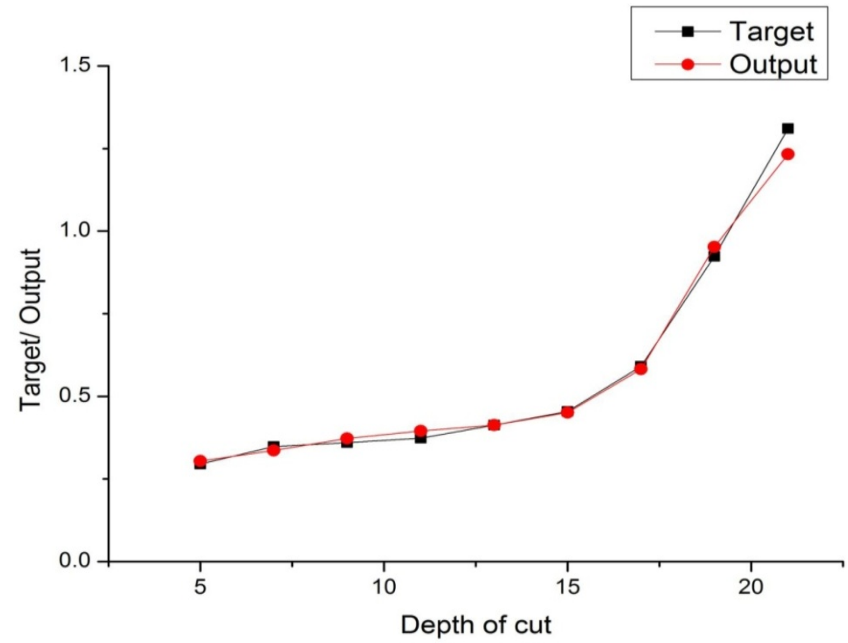

Figure 4.5: Graph of Actual result versus Output result

Table 4.6: Summary

	Target	**Output**	**AE**	**ARE**
Mean	0.563111	0.559961	0.019186	0.030061
Std Dev	0.319523	0.301437	0.022085	0.019451
Min	0.295	0.304454	0.000102	0.000246
Max	1.31	1.232731	0.077269	0.059048

Based on the analysis obtain, the correlation was 0.997307 and the R-squared was 0.990581

Table 4.7: Prediction of surface roughness

Depth of cut	**Ra**
6	0.317563
8	0.356072
10	0.385446
12	0.40339
14	0.426865
16	0.495972
18	0.737947
20	1.135358
22	1.272533
24	1.294917
26	1.299579
28	1.300844
30	1.301229
32	1.301351
34	1.301391
36	1.301403
38	1.301407
40	1.301409
42	1.301409
44	1.301409
46	1.301409
48	1.301409
50	1.301409

4.4.2 Multi Pass

Table 4.8: Target and Output Result obtain using neural network

	Row	Depth of cut	Target	Output	AE	ARE
VLD	0	5	0.195	0.204944	0.009944	5.099298
TRN	1	7	0.205	0.205058	0.000058	0.028326
TRN	2	9	0.218	0.218003	0.000003	0.001268
TST	3	11	0.238	0.252784	0.014784	6.211891
TRN	4	13	0.259	0.258559	0.000441	0.17043
TRN	5	15	0.274	0.274972	0.000972	0.35492
TRN	6	17	0.306	0.304688	0.001312	0.428833
TRN	7	19	0.318	0.320987	0.002987	0.939427
TRN	8	21	0.327	0.324431	0.002569	0.785495

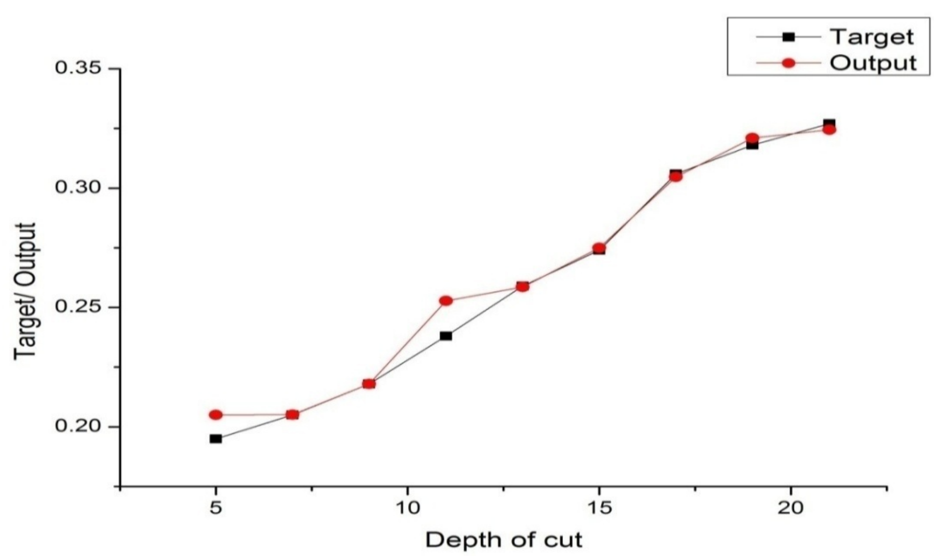

Figure 4.6: Graph of Actual result versus Output result

Table 4.9: Summary

	Target	Output	AE	ARE
Mean	0.26	0.262714	0.003675	0.015578
Std Dev	0.046743	0.044589	0.00488	0.022259
Min	0.195	0.204944	0.000003	0.000013
Max	0.327	0.324431	0.014784	0.062119

Based on the analysis obtain, the correlation was 0.993928 and the R-squared was 0.981231

Table 4.10: Prediction of surface roughness

Depth of cut	Ra
6	0.20496
8	0.206132
10	0.245826
12	0.255114
14	0.264707
16	0.289483
18	0.31548
20	0.323391
22	0.324905
24	0.325244
26	0.32533
28	0.325353
30	0.325359
32	0.325369
34	0.325380
36	0.325415

38	0.325419
40	0.325421
42	0.325421
44	0.325421
46	0.325421
48	0.325421
50	0.325421

Figure 4.7 show that the prediction for surface roughness according to different depth of cut (6-50µm). Table 4.7 shows the result of roughness prediction for single pass and table 4.10 show the prediction result for multi pass. The neural network software was used to analyze the summary and to predict the surface roughness. Based on the analysis, the surface roughness value for prediction for both experiment increased. This clearly shows that when there is an increase in depth of cut, the surface roughness also will be increase. The graph above show that at 1 point the graph will be remain constant. According to table 4.6, it shows the summary for overall analysis in single pass experiment. The mean obtained for target value is 0.563111 µm while for output is 0.559961 µm. Based on the analysis obtain for single pass experiment, the correlation was 0.997307 and the R squared was 0.990581. According to table 4.9, it shows the summary for multi pass experiment. The mean obtained for target value is 0.26 µm while for output value is 0.262714 µm. Based on the analysis obtain for multi pass experiment, the correlation was 0.993928 and the R-squared was 0.981231.

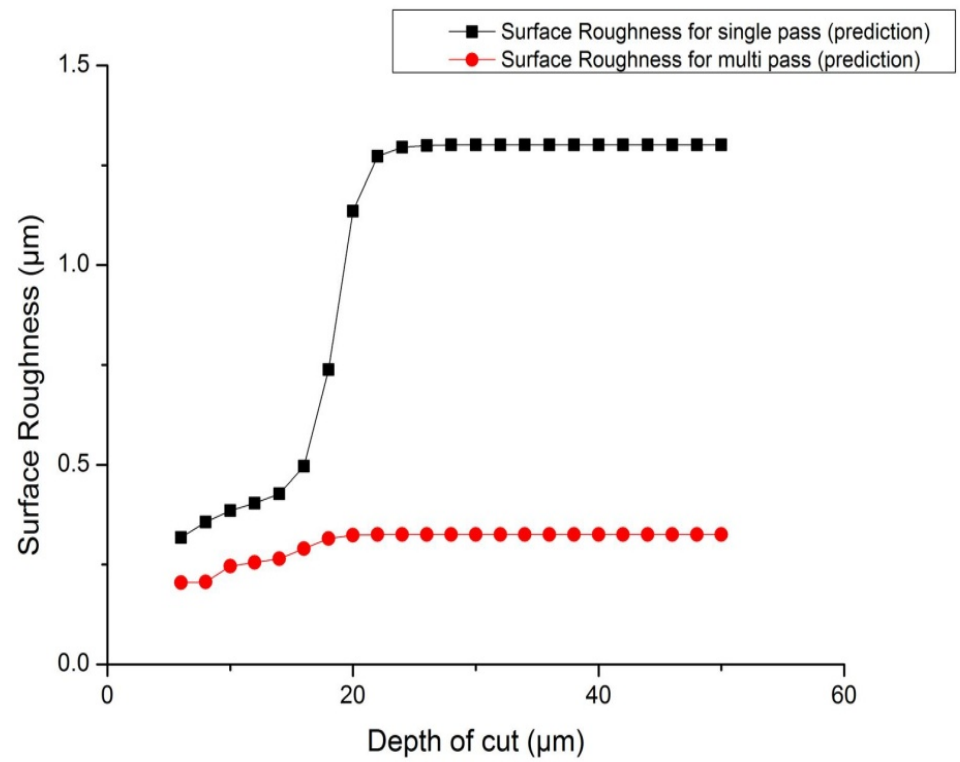

Figure 4.7: Surface roughness for single pass and multi pass for prediction depth of cut.

CHAPTER 5

CONCLUSION

5.1 INTRODUCTION

This chapter mainly discuss about the conclusions that can be derived from this experiment. Besides that, it also suggests some future recommendations for the purpose of further studies in the field of grinding process.

5.2 CONCLUSION

The relation between the surface roughness, wheel wear and depth of cut for both experiment were studied along this project. We observed that as the depth of cut increases, the surface roughness also increases. The surface roughness obtained for single pass is higher than the multi pass experiment. For example, for depth of 5µm the surface roughness obtained for single pass is 0.295µm while for multi pass the roughness obtained is 0.195 µm. We also studied about the wheel wear produced along the experiment. There is no changes in wheel diameter thus there is no wheel ratio. The microstructure observation shows that the material surfaces for single pass are rough compare to multi pass with the increase in depth of cut.

As overall conclusion, the optimum parameter obtained during the experimental is 5µm. Neural Network has been developed to find out prediction model of surface roughness until cutting depth 50µm. Besides that, from overall study we can see that the results of surface roughness using Titanium Oxide are much better compare to water based coolant. For example in single pass experiment for the depth of cut (5µm), the surface roughness obtained when using Titanium Oxide Nanocoolant is 0.295µm compare to water based coolant result which is 0.35µm.

5.3 FUTURE RECOMMENDATIONS

In future, we can use various concentration of nanocoolant. We can compare the relationship and the result between different kinds of concentration. Besides that, we can conduct the experiment using different kind of passes and using various depth of cut. For this experiment, we using Haynes 242 as material of work piece so for further investigation, we can test the experiment using different types of material.

REFERENCES

[1] Emmanuel C. Nsofor, 2008. *Recent Patents on Nanofluids (Nanoparticles in Liquids)Heat Transfer, 1,* 190-197

[2] Turgut. A, Tavman.I, Chirtoc. M , Schuchman. H.P , Sauter. C and Tavman. S, 2009 *Thermal Conductivity and Viscosity Measurements of Water Based* TiO_2 *Nanofluids, 3*0:1213–1226

[3] Jing .Y.Z, Steven Y. L, Jun Yao, Jia M.C and Jing L.H, 2006, *Evolutionary optimization of machining processes*, 17:203–215

[4] Kopac. J, Krajnik. P , 2006, *High-performance grinding A review*, Journal of Materials Processing Technology, 278–284

[5] Stephen D. Antolovich, Dwaine L. Klarstrom and John F, 2000. *The Ductility of Haynes 242 Alloy as a Function of Temperature, Strain Rate and Environment*

[6] Singh. A.K, 2008. *Thermal Conductivity of Nanofluids*, Defence Institute of Advanced Technology, Pune-411 025

[7] Stephen U. S. Choi, 2009. *Nanofluids: From Vision to Reality Through Research*, Chicago, IL 60607

[8] Halil D, Abdulkdir. G and Ibrahim. C, 2010, *An Investigation into the Influences of Grain Size and Grinding Parameters on Surface Roughness and Grinding Forces when Grinding,* 447-454

[9] Viktor. P. Astakhov, 2006, *Effects of the cutting feed, depth of cut, and work piece (bore) diameter on the tool wear rate,* Production Service Management Inc

[10] Nazwa. T and Hashim.U, 2010, *Precision Surface Grinding Of Silicon Carbide With Fine Grain Diamond Cup Wheel*, Engineering e-Transaction (ISSN 1823-6379)